Functionalized Mesoporous Silica Iron Oxide Nanoparticles for Thermal Therapy and T_1 Contrast

Hattie L. Ring[1,2], Katie R. Hurley[2], Michael Etheridge[3,4], Jinjin Zhang[1,5], Nathan D. Klein[2], Connie Chung[3,4], Qi Shao[4], John C. Bischof[3,4], Christy L. Haynes[2], and Michael Garwood[1,6]

[1]*Center for Magnetic Resonance Research, University of Minnesota, Minneapolis, MN, United States,* [2]*Chemistry, University of Minnesota, Minneapolis, MN, United States,* [3]*Mechanical Engineering, University of Minnesota, Minneapolis, MN, United States,* [4]*Biomedical Engineering, University of Minnesota, Minneapolis, MN, United States,* [5]*Physics, University of Minnesota, Minneapolis, MN, United States,* [6]*Radiology, University of Minnesota, Minneapolis, MN, United States*

Introduction: Iron oxide nanoparticles (IONPs, Ferrotec EMG-308) offer an attractive platform for combinatorial cancer therapies, because of their heating characteristics, drug loading capability, and utility as T_2, T_2^*, or T_1 contrast agent. However, these qualities may become substantially altered or diminished when placed in biological suspensions due to aggregation[1]. For example, when exposed to buffers or LNCaP prostate cancer cells, the specific absorption rate (SAR) in RF-induced magnetic fluid hyperthermia drops to 50% of the original value, the longitudinal ($R_1=1/T_1$) relaxivity drops even further (~70% lower than original)[1], and quantification is difficult with T_2^* weighted MRI. Positive contrast for detecting of IONPs, can be obtained with T_1-weighted sequences that have no echo time (TE=0), like sweep imaging with Fourier transform (SWIFT)[4]. Such sequences provide a means to quantify IONP uptake *in vivo*. We show that mesoporous silica coating provides many benefits, most importantly, a resistance to biological aggregation[2,3] and positive T_1 contrast visualization *in vivo*.

	IONP	msIONP
SAR (W/g Fe)	244.4 ± 14.9	203.9 ± 7.1
r_1, 9.4T ($mM^{-1}s^{-1}$)	0.89 ± 0.01	0.16 ± 0.02
r_2, 9.4T ($mM^{-1}s^{-1}$)	178.1 ± 12.9	109.5 ± 1.17
r_1, 1.4T ($mM^{-1}s^{-1}$)	20.8 ± 0.7	7± 0.1
r_2, 1.4T ($mM^{-1}s^{-1}$)	333± 3	267± 4

Table 1: The SAR, r_1, and r_2 for IONPs and msIONPs. Relaxivity measurements were made at 9.4T and 1.4T.

Methods: Unmodified and PEG-functionalized mesoporous silica-coated IONPs (msIONPs) properties were compared and then characterized in biologically relevant environments including phosphate buffered saline (PBS), lymph node carcinoma of prostate (LNCaP) cells, and after direct injection into LNCaP prostate cancer tumors in nude mice. SAR was determined by measuring temperature change under an alternating magnetic field generated by a home-built 3-loop coil with alternating current[1]. Relaxivity measurements at 1.4T were performed with a Bruker Minispec mq60 NMR Analyzer at 60 MHz. T_1 relaxation values were obtained via an inversion recovery sequence. T_2 relaxation values were obtained with a Carr-Purcell-Meiboom-Gill sequence. Both measurements were performed at 37°C on solutions with low mM iron concentrations. The relaxation rates were measured in 1% agar suspensions at 9.4T. T_1 was measured with the SWIFT Look-Locker method[5], while linewidth measurements were used to calculate T_2. Colloidal stability was compared by suspending both nanoparticles in PBS of various salinities at room temperature and using dynamic light scattering (DLS) to observe changes in the hydrodynamic diameter over 4 hours. Cellular uptake was investigated by transmission electron microscopy (TEM) after incubating a concentration of 0.5 mg Fe/mL IONPs and msIONPs in an LNCaP cell line for 24 hours. Lastly, *in vivo* measurements were performed on hindlimb LNCaP tumors with IONPs and msIONPs directly injected at 0.5 mg Fe/g tumor. The location of the nanoparticles was revealed with SWIFT MRI[4] and the T_1 map was acquired using the SWIFT Look-Locker method[5,6]. All SWIFT measurements were made on a 9.4T animal MRI scanner (Agilent Technolgies, USA).

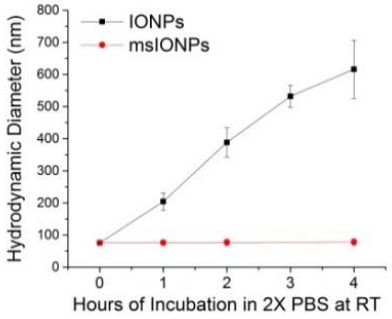

Figure 1: IONPs in high concentrations of PBS begin to aggregate within one hour, reaching aggregates of ~700nm hydrodynamic diameter after four hours. In contrast, msIONPs do not aggregate over four hours.

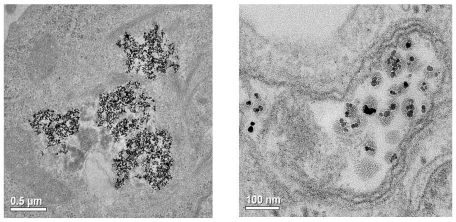

Figure 2: Endosome uptake of (left) IONPs and (right) msIONPs in LNCaP cells. IONPs form 'super-aggregates', while msIONPs are taken up infrequently and in much smaller groups.

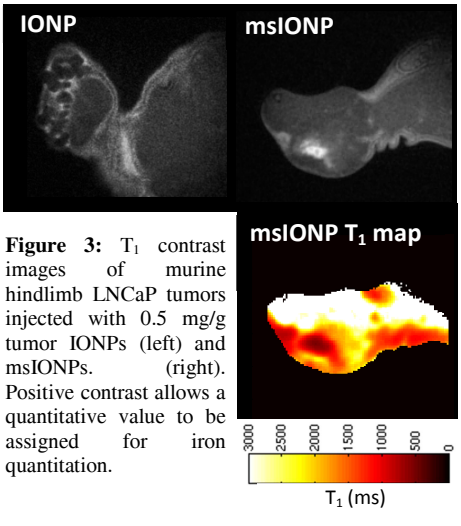

Figure 3: T_1 contrast images of murine hindlimb LNCaP tumors injected with 0.5 mg/g tumor IONPs (left) and msIONPs. (right). Positive contrast allows a quantitative value to be assigned for iron quantitation.

Results: Once coated, IONPs maintained colloidal stability (figure 1) along with maintenance of high heating (SAR is lowered by only 17% vs. up to 100% when aggregated) and high relaxivity behaviors in biological environments. As is shown in figure 2, the IONPs are in aggregates comprised of thousands of individual IONPs, whereas, the msIONPs have far less uptake. Although SWIFT has been shown to allow accurate quantitation of IONPs up to 3 mg/mL in agarose phantoms[5], the complexity of the *in vivo* system and the high regional concentration of IONPs contribute to the dipole artifact shown in figure 3. In contrast, injection with the same iron dose (0.5 mg/g tumor) of msIONPs displays a bright region which allows analysis of the iron distribution.

Discussion: Colloidal stability and minimal non-specific cell uptake allowed for effective heating in biological suspensions and strong signal enhancement in T_1-weighted MR imaging *in vivo*. The *in vitro* studies indicated that the msIONPs remain largely outside the cells and well-separated from one another. The colloidal stability and lower cell uptake minimizes the artifacts in MRI images. Ongoing work will focus on *in vivo* calibration curves to relate msIONP T_1 values with SAR.

Conclusions: Visualization of magnetic nanoparticles was achieved by utilizing both SWIFT MRI and an even distribution of non-aggregated particles.

Acknowledgements: This work is supported by the University of Minnesota (UM Futures and Institute for Engineering Medicine Seed Grants), the NSF/CBET(1066343 and 1133285), and the NIH (P41 EB015894).

References: (1) M. L. Etheridge, *et. al.*, *Technology*, 2014, **02**, 214-228. (2) Y.-S. Lin, *et. al.*, *Chem. Comm.*, 2011, **47**, 532-534. (3) Y.-S. Lin, *et. al.*, *JACS*, 2011, **133**, 20444-20457. (4) D. Idiyatullin, *et. al.*, *JMR*, 2006, **181**, 342-349. (5) J. Zhang, *et. al.*, *MRM*, 2014, **71**, 1982-1988. (6) J. Zhang, et. al., *ISMRM*, 2015.